The role of desmoplakin for neuronal function in the dentate gyrus and anxiety-related behavior

Keisuke Otsubo[a,#], Naoko Sakashita[a,#], Yuki Nishimoto[a,#], Yo Sato[a], Katsunori Kobayashi[b], Kanzo Suzuki[a], Eri Segi-Nishida[a,*]

[a]Department of Biological Science and Technology, Faculty of Advanced Engineering, Tokyo University of Science, Tokyo, Japan

[b] Department of Pharmacology, Graduate School of Medicine, Nippon Medical School, Tokyo 113-8602, Japan

[#] these authors equally contributed to this work

*Correspondence to:

Eri Segi-Nishida,

6-3-1 Niijuku, Katsushika-ku, Tokyo, Japan, 125-8585

Email: eri.segi.nishida@rs.tus.ac.jp

Running title: Role of desmoplakin in DG

Abstract

Desmoplakin (Dsp) is a component of desmosomal cell-cell junctions that interacts with the cadherin complex and cytoskeletal intermediate filaments. In addition to its function as an adhesion component, Dsp is involved in various biological processes, such as gene expression, differentiation, and migration. Dsp is specifically expressed in the hippocampal dentate gyrus (DG) in the central nervous system. However, it is unclear how Dsp impacts hippocampal function and its related behaviors. Using an adeno-associated virus knockdown system in mice, we provide evidence that Dsp in the DG maintains hippocampal functions, including neuronal activity and adult neurogenesis, and contributes to anxiolytic effects. Dsp protein is mostly localized in mature granule cells in the adult DG. Dsp knockdown in the DG resulted in a lowered expression of an activity-dependent transcription factor FosB, and an increased expression of mature neuronal markers, such as calbindin. In addition, the suppression of Dsp decreases serotonin responsiveness at the DG output mossy fiber synapses and impairs adult neurogenic processes in the subgranular zone of the DG. Moreover, DG-specific Dsp knockdown mice showed an increase in anxiety-like behaviors. Taken together, this research uncovers an unexplored function for Dsp in the central nervous system and suggests that Dsp in the DG may function as a regulator to maintain proper neuronal activation and contribute to the adaptation of emotion-related behavior.

Keywords: anxiety; dentate gyrus; desmoplakin; hippocampus; knockdown; neurogenesis

Introduction

Desmosomes are adhesive intercellular junctions that provide strong adhesion between cells and are abundant in tissues exposed to mechanical stress, such as the heart and skin. Mutations in these factors cause skin and heart vulnerability (Kowalczyk and Green, 2013). Desmosomal components comprise transmembrane cadherins, such as desmoglein and desmocollin, and intracellular proteins, such as plakoglobin, plakophilin, and desmoplakin (Dsp) (Garrod and Chidgrey, 2008; Broussard et al., 2015). Dsp is a family of plakin proteins that interacts with the cadherin/plakoglobin/plakophilin complex through the N-terminal domain and with an intermediate filament cytoskeleton through the C-terminal domain (Delva et al., 2009). In addition to mediating cell-to-cell adhesion, desmosomes function as cell signaling regulators involved in cell proliferation and differentiation (Johnson et al. 2014). In particular, Dsp is involved in processes such as gene expression, differentiation, and microtubule dynamics, indicating its diverse biological functions in addition to its function as an adhesion component (Bendrick et al., 2018; Dubash et al., 2016; Lombardi et al., 2016; Patel et al., 2014).

In the central nervous system, Dsp is specifically expressed in the hippocampal dentate gyrus (DG) in the brain (Yamasaki et al., 2008). The DG gates the flow of neocortical information into the hippocampal CA3 region. The DG is one of the few areas of the mammalian brain where adult neurogenesis occurs (Drew et al., 2013; Zhao et al., 2008). Neurogenesis is a multi-step process consisting of proliferation, differentiation, survival, and maturation and is regulated by various factors, including signals from adjacent granule cells (Kempermann et al., 2015). The neurogenic region in the DG is the subgranular zone (SGZ), which is adjacent to the mature granule cell layer. It has been reported that Dsp is characterized as a molecular maker for neuronal

68 maturation in the DG of hippocampus (Kobayashi et al., 2010). The expression level of
69 *Dsp* in the DG increases with postnatal development, similarly to the patterns of other
70 DG maturation markers, calbindin and tryptophan-2,3-dioxygenase 2 (Tdo2). Dsp
71 transcription is directly regulated by Bcl11b, a transcription factor that plays an
72 important role in postnatal development of the DG (Simon et al., 2012). Forebrain
73 neuron-specific knockout of Dsp in Emx1-Cre mice impairs progenitor proliferation
74 and neuronal differentiation at 14 days postnatal age, indicating that Dsp contributes to
75 the development of DG neurons (Simon et al., 2012). However, whether Dsp regulates
76 the function of mature DG neurons and the mechanisms through which Dsp affects the
77 process of adult neurogenesis in the neighboring SGZ region remain unclear.

78 The hippocampus is a limbic structure implicated in the regulation of stress and
79 pathophysiology/treatment of anxiety and depression (Segi-Nishida and Suzuki, 2022).
80 We have previously demonstrated that long-term antidepressant treatment suppresses
81 the expression of *Dsp* in the DG, indicating that Dsp may be an important molecule in
82 antidepressant effect (Kobayashi et al., 2010; Imoto et al., 2017). Neuron-specific
83 knockout mice of norbin, a known G-protein regulator, show depression-like behavior
84 and decreased expression of *Dsp* in the DG. These previous studies indicate that Dsp
85 plays a key role in emotion-related behaviors in the DG. Nevertheless, whether Dsp in
86 the DG during adulthood is involved in emotion-related behaviors such as depression
87 and anxiety is unclear.

88 In this study, we investigated the effect of Dsp knockdown in the DG on
89 neuronal activation, adult hippocampal neurogenesis, and emotion-related behaviors
90 using an adeno-associated virus (AAV) knockdown system. We found that Dsp in the
91 adult hippocampal DG maintains the function of DG neurons, regulates neuronal

differentiation during adult neurogenesis, and behaviorally contributes to anxiolytic effects.

Materials and Methods

Experimental animals

Seven-to-eight-week-old male C57BL/6N mice (23–25 g) were purchased from Japan SLC (RRID5295404; Hamamatsu, Japan). The mice were housed in groups of six per cage (32 cm length × 11 cm width × 13.5 cm height). All the mice were housed under standard conditions (temperature: 24 ± 2 °C, humidity: 55% ± 5%) with a 12 h light/dark cycle and *ad libitum* access to water and food (MR standard, Nosan Corporation, Yokohama, Japan). The weight gain of each mouse was recorded during the experiments to monitor their physical condition. All mice were habituated for longer than one week before the experimental procedures were performed. Animal use and procedures were conducted in according the Tokyo University of Science regulations on animal care and use in research and were approved by the Animal Care and Use Committee of Tokyo University of Science (approval numbers K20009, K21007, and K22007).

AAV preparation and hippocampal administration

AAVs (serotype rh10) expressing artificial microRNAs (miRNAs) targeting Dsp or control miRNAs with Emerald Green Fluorescent Protein (EmGFP) under the EF1α promoter were generated as follows: We designed the sequences for artificial microRNAs for Dsp according to the BLOCK-iT RNAi Designer website (Thermo Fisher Scientific). First, the DNA fragment encoding miRNA for *Dsp* (5'-TGC TGT TGA GAT GGA CAT CAA TGC ACG TTT TGG CCA CTG ACT GAC GTG CAT

TGG TCC ATC TCA A-3' and 5'-CCT GTT GAG ATG GAC CAA TGC ACG TCA GTC AGT GGC CAA AAC GTG CAT TGA TGT CCA TCT CAA C-3') was subcloned into pcDNA6.2-GW-EmGFP-miR using BLOCK-iT Pol II miR RNAi Expression Vector Kit (Invitrogen). The EmGFP and Dsp miRNA fragments were amplified by PCR from this vector and inserted between the KpnI and EcoRV sites of the pAAV-EF1α-DIO EYFP vector (#27056; Addgene). The resulting plasmid was named pAAV-EF1α-EmGFP-miR-Dsp. The DNA fragment encoding control microRNA (5′-TGC TGA AAT GTA CTG CGC GTG GAG ACG TTT TGG CCA CTG ACT GAC GTC TCC ACG CAG TAC ATT T-3′ and 5′-CCT GAA ATG TAC TGC GTG GAG ACG TCA GTC AGT GGC CAA AAC GTC TCC ACG CGC AGT ACA TTT C-3′), which can form a hairpin structure processed into mature microRNA but is predicted not to target any known vertebrate gene, was used to generate an AAV vector expressing control microRNA. TheBLOCK-iT Pol II miR RNAi Expression Vector Kit was used instead of those encoding Dsp miRNA. AAV particles were produced using the previously described procedure with minor modifications (Shinohara et al., 2018). Briefly, the AAVrh10 expression plasmid (Addgene #112866), pHelper vector (#240071, Agilent Technologies, Santa Clara, CA), and the constructed AAV-vector plasmid were transfected into AAV-293 cells (#240073, Agilent) using Lipofectamine 2000 (Thermo Fisher Scientific). Transfected AAV-293 cells were collected 72 h after transfection, resuspended in artificial cerebrospinal fluid, frozen, and thawed three times. Cell debris was eliminated by centrifugation at 10,000 × g for 10 min and the supernatant containing the virus was collected. The viral suspension was incubated with benzonase (Merck Millipore, Burlington, MA, USA) to degrade residual DNA. The prepared AAV solution was aliquoted and stored at -80 °C. The AAV titer was quantified using PCR (5′-TGA GTC ACC CAC ACA AAG GA-3′ and 5′-CCA AGC

142 TGG CCT AAC TTC AG-3′) after proteinase K treatment (Merck Millipore). Under
143 anesthesia with a mixture of medetomidine (0.3 mg/kg, ZENOAQ, Japan), midazolam
144 (4 mg/kg, Sandoz, Japan), and butorphanol (5 mg/kg, Meiji, Japan), the mouse brain
145 was fixed with stereotaxic instruments (Narishige, Tokyo, Japan). An AAV solution of
146 500 nL per injection site (5.0×10^8 copies) was stereotaxically injected at two sites in
147 each hemisphere into the DG using a PV-820 Pneumatic PicoPump (World Precision
148 Instruments, Hessen, Germany) through a glass micropipette made with a PN-30
149 micropipette puller (Narishige). The stereotaxic coordinates were targeted to the ventral
150 DG: 3.2 mm posterior to the bregma, 2.7 mm lateral to the midline, and 3.0 mm ventral
151 to the skull surface at the bregma, according to the mouse brain atlas (Paxinos and
152 Franklin, 2012). Data were excluded from the analysis if fluorescence was not observed
153 in the DG.
154
155 **Electroconvulsive stimulation and drug treatment**
156 Bilateral ECS (current, 25–35 mA; shock duration, 1 sec; frequency, 100 pulse/sec;
157 pulse width, 0.5 msec) was administered with a pulse generator (ECT Unit; Ugo Basile,
158 VA, Italy) to mice as described previously (Imoto et al., 2017). ECS was administered
159 4 times a week. Fluoxetine hydrochloride (LKT Labs, St. Paul, MN, USA) was
160 dissolved in drinking water and orally applied at a dose of 22 mg/kg/day for 4 weeks
161 as described previously (Kobayashi et al., 2010).
162
163 **RNA extraction and real-time PCR**
164 Seven to eight weeks after AAV infection, the mice were decapitated under deep
165 anesthesia, coronal brain slices (1 mm) were cut using a tissue slicer, and the DG of the
166 hippocampus was dissected. Total RNA was extracted using the Reliaprep RNA Cell

167 Miniprep System (Promega, Madison, WI, USA) and reverse transcribed using
168 ReverTra Ace (Toyobo, Osaka, Japan). Subsequent, real-time PCR was performed
169 using the StepOne system (Applied Biosystems, Foster City, CA) and Thunderbird
170 SYBR qPCR mix (Toyobo). The expression levels of each gene were quantified using
171 standardized external dilutions. The relative expression levels of the target genes were
172 normalized to those of 18S rRNA or *Gapdh*. The specificity of each primer set was
173 confirmed by melt-curve analysis, and the product size was examined using gel
174 electrophoresis. Table 1 summarizes the primer sequences for each gene.
175
176 **Electrophysiological analysis**
177 Mice were decapitated under deep anesthesia 7–8 weeks after AAV infection, and both
178 hippocampi were isolated. Transverse hippocampal slices (380 μm) were cut in ice-cold
179 saline using a tissue slicer (7000smz, Campden Instruments Ltd., Leics, UK). The slices
180 were then incubated for 30 min at 30 °C and maintained in a humidified interface-
181 holding chamber at room temperature before use. Intense GFP fluorescence in the DG
182 and the mossy fiber (MF) tract was confirmed, and electrophysiological recordings
183 were performed as described (Kobayashi et al., 2010, 2020). Electrophysiological
184 recordings were made in a submersion-type chamber maintained at 27.0–27.5 °C and
185 superfused at 2 mL/min with recording saline composed of (in mM): NaCl, 125; KCl,
186 2.5; NaH2PO4, 1.0; NaHCO3, 26.2; glucose, 11; CaCl2, 2.5; MgCl2, 1.3 (equilibrated
187 with 95% O2 / 5% CO2). Field excitatory postsynaptic potentials (EPSPs) arising from
188 the MF synapses were evoked by stimulating the dentate granule cell layer with bipolar
189 tungsten electrodes and were recorded from the stratum lucidum of CA3 using a glass
190 pipette filled with 2 M NaCl. The amplitude of field EPSPs was measured with a 0.5-
191 ms window positioned at 70–80% of the peak of the baseline field EPSPs. More than

192 85% block of EPSP by an agonist of group II metabotropic glutamate receptors
193 (2*S*,2'*R*,3'*R*)-2-(2',3'-dicarboxycyclopropyl) glycine (DCG-IV, 1 μM) was the criterion
194 used to identify MF input. A single electrical stimulation was delivered at a frequency
195 of 0.05 Hz. The initial slope of the EPSPs was measured through analysis. All
196 recordings were performed using a Multiclamp 700 B amplifier (Molecular Devices,
197 Sunnyvale, CA, USA), filtered at 2 kHz, and stored on a personal computer via an
198 interface (digitized at 10 kHz). Data were obtained from distinct samples. Serotonin
199 hydrochloride was purchased from Sigma-Aldrich.
200
201 **Sample isolation for immunohistochemistry**
202 Five'-bromo-2'-deoxyuridine (BrdU, 150 mg/kg, Nacalai Tesque, Japan) was
203 intraperitoneally administered to mice once 2 h before sacrifice to evaluate cell
204 proliferation to label the dividing cells, or four times on 14 and 15 days (twice a day)
205 before sacrifice to evaluate cell survival.
206 For Dsp immunostaining, the mice were deeply anesthetized and transcardially
207 perfused with cold saline. The brains were then stored at -80°C until further use. Serial
208 fresh frozen sections (18 μm thick) were cut through the entire hippocampus using a
209 cryostat (Leica 1510, Leica Microsystems, Wetzlar, Germany) and stored at -80°C. For
210 other immunostaining procedures, mice were deeply anesthetized and perfused with
211 cold saline followed by 4% paraformaldehyde in 0.1 M phosphate buffer (pH 7.4) and
212 were post-fixed at 4 °C for 48 h. The brains were then cryoprotected in 20% sucrose
213 for 48 h and in 30% sucrose for 24 h and stored at -80°C until further use. Serial sections
214 (30 μm thick) were cut through the entire hippocampus using a cryostat and stored in
215 30% glycerol and 30% ethylene glycol in 0.02 M phosphate buffer (pH 7.4) at -20 °C
216 until staining.

217

218 **Immunohistochemistry**

219 For Dsp or Dsp/NeuN immunostaining, fresh frozen sections were fixed with 100%
220 methanol for 20 min at 4 °C. After fixation, the sections were washed with phosphate-
221 buffered saline (PBS), blocked using 10% equine serum in PBS, and incubated with
222 monoclonal mouse anti-Dsp (1:50; Progen, 61003, RRID:AB_2920666), rabbit anti-
223 NeuN (1:1000, Abcam, ab177487, RRID:AB_2532109) at 4 °C overnight. After
224 washing with PBS, the sections were incubated with donkey anti-mouse IgG antibodies
225 conjugated to Alexa Fluor 647 (1:300; Thermo Fisher Scientific, RRID:AB_162542)
226 and donkey anti-rabbit IgG antibodies conjugated to Alexa Fluor 555 (1:1000; Thermo
227 Fisher Scientific, RRID:AB_2535853) for 60 min. The sections were then incubated
228 with 4',6-diamidino-2-phenylindole (DAPI; 1:10,000; Merck Millipore) and mounted
229 on slides with Mowiol (Merck Millipore) after washing with PBS.

230 For FosB, NeuroD1, and doublecortin (DCX) immunostaining, the 30 μm thick
231 floating sections were washed with PBS and blocked using 10% equine serum
232 (SH30074; Cytiva) in PBS containing 0.3% Triton X-100 (PBST) at room temperature
233 for 60 min, followed by overnight incubation with rabbit anti-FosB (1:1000; Abcam,
234 ab184938, RRID: AB_2721123), rabbit anti-NeuroD1 (1:1000; Abcam, ab213725,
235 RRID:AB_2801303), rabbit anti-doublecortin (DCX) (1:1000; Cell Signaling
236 Technology, Danvers, MA, USA; RRID:AB_561007) at 4 °C. For BrdU
237 immunostaining, the floating sections were incubated in 50% formamide in 2×saline
238 sodium citrate buffer (SSC) for 2 h at 60 °C, followed by incubation in 2 M hydrogen
239 chloride at 37 °C for 30 min, and neutralized with 0.1 M boric acid (pH 8.5) at room
240 temperature for 10 min before blocking. After blocking, the sections were incubated
241 overnight with monoclonal rat anti-BrdU (1:8000; Abcam, ab6326, RRID:AB_305426)

242 at 4°C. After washing with PBST, the sections were incubated with donkey anti-rabbit
243 IgG antibody conjugated to Alexa Fluor 555 (1:1000 for NeuroD1 and FosB
244 immunostaining; Thermo Fisher Scientific, RRID:AB_2535853) and donkey anti-rat
245 IgG antibody conjugated to Alexa Fluor 555 (1:1000 for BrdU immunostaining;
246 Abcam, RRID: AB_2813834) for 60 min. After washing with PBST, the sections were
247 incubated with DAP (1:10000) and mounted on slides with Mowiol after washing with
248 PBS. For DCX immunostaining, the sections were incubated with biotinylated goat
249 anti-rabbit IgG (1:200; Vector Laboratories Inc., Burlingame, CA, USA; BA1000,
250 RRID: AB_2313606) for 60 min. The sections were washed with PBST and incubated
251 with the ABC Vectastain Kit (Vector), and antigen detection was performed with 0.06%
252 3,3'-diaminobenzidine (Wako) staining. After washing, the sections were mounted on
253 slides using Entellan New (Merck Millipore).
254
255 **Quantification of BrdU-, NeuroD1-, DCX-, and FosB-positive cells**
256 Computer-assisted image analysis (ImageJ, NIH, Bethesda, MD, USA; QuPath,
257 Bankhead et al., 2017) was used for cell analysis. For quantification of FosB-positive
258 cells, three sections of DG-expressing EmGFP were photographed under a microscope
259 (BZX-700, Keyence, Osaka, Japan). The number of FosB-positive cells was counted
260 and presented as the number of cells per 10,000 μm^2 area in the granule cell layer of
261 the DG. For BrdU-labeled cell quantification, 6–8 sections of DG-expressing EmGFP
262 were photographed under a microscope. To evaluate cell proliferation, the number of
263 BrdU-positive cells was counted in the SGZ and presented as the number of cells per
264 1,000 μm along the SGZ. To evaluate cell survival, the number of BrdU-positive cells
265 in the granule cell layer of the DG was counted and presented as the number of cells
266 per 100,000 μm^2 of the granule cell layer. For NeuroD-positive cell quantification, four

267 sections of the DG expressing EmGFP were photographed using a microscope. The
268 number of NeuroD1-positive cells in the SGZ was counted and presented as the number
269 of cells per 1,000 μm along the SGZ. For DCX-positive cell quantification, 2–3 sections
270 of DG-expressing EmGFP were photographed using a microscope. DCX-positive cells
271 in which dendrites reached the molecular layer and underwent complex processes were
272 subcategorized as DCX-positive cells with long and branched dendrites. The total
273 number of DCX-positive and DCX-positive cells with long dendrites was counted in
274 the SGZ and presented as the number of cells per 100 μm along the SGZ.
275
276 **Behavioral experiments**
277 The mice were habituated to the testing room for at least 30 min before the behavioral
278 test. During the test, the movement of each mouse was recorded using a digital video
279 camera. All records were stored and analyzed using the SMART 3.0 video tracking
280 software (Panlab, Barcelona, Spain, RRID: SCR_002852). The apparatus was
281 thoroughly cleaned with 70% ethanol after the removal of each mouse. The time course
282 of each experiment is shown in Fig. 6A.
283 The open field test (OFT) was performed for 10 min using an apparatus
284 composed of opaque white walls and a floor (50 cm × 50 cm × 20 cm) illuminated at
285 an intensity of 80 lux in the center of the floor. Each mouse was placed in the center of
286 an open-field arena, and locomotor activity was recorded for 10 min. The total distance
287 moved, relative time spent in the central zone, and entry time into the central zone were
288 measured. The floor was divided into 25 squares, and the four central squares were
289 defined as the central zone.
290 The forced swim test (FST) was performed in a cylindrical container (13 cm
291 diameter, 25.5 cm height) filled with water to a height of 18 cm. Water (23–25 °C) was

replaced between the trials. The FST was performed and recorded for 10 min using a digital video camera. The duration of immobility was then quantified.

The spontaneous locomotor activity (LMA) test was performed in a transparent home cage without bedding (20 cm length × 12.5 cm width) over 60 min. The total distance moved during the last 30 min was tracked.

The compartment social interaction test (SIT) was performed in an SIT apparatus (LE894T, Panlab) consisting of three chambers (42 cm × 60 cm × 22 cm) and two partitions (5.5 cm × 0.15 cm × 17 cm). Each mouse was placed in the middle chamber and allowed to explore the chamber freely for 5 min. Immediately after habituation, an unfamiliar mouse (a 7–8-week-old male C57BL/6N mouse) was introduced into one of the two side chambers enclosed in a wire cage. An identical empty wire cage was placed on the opposite side of the chamber. After placement, the side doors were opened simultaneously, and the test mouse was allowed to explore the entire three-chamber arena for 10 min. The time spent in each compartment was measured.

An elevated plus maze (EPM) test was performed in an EPM apparatus (EPM-X, Muromachi Kikai, Japan) consisting of two open arms (30 cm × 6 cm, 40 lux) and two closed arms (30 cm × 6 cm × 15 cm, 20 lux) extending from a central platform (6 cm × 6 cm). The maze was elevated to 40 cm above the floor. Each mouse was placed in the center of the maze, facing the open arm, and allowed to explore freely for 10 min. The total distance and time spent in the open arms were measured using Smart 3.0.

Statistical analyses

All data are presented as the mean ± standard error of the mean. Statistical analyses were performed using an unpaired Student's *t*-test, Welch's *t*-test, or two-way analysis

of variance (ANOVA). Statistical significance was set at $P < 0.05$. Before performing *t*-test, normality of the data was examined using the Shapiro–Wilk test. If the data did not pass the normality test, a nonparametric test, the Mann–Whitney U test, was performed. Detailed statistical data are presented in Supplementary Table 1 (Table S1). All analyses were performed using the PRISM 9 software (GraphPad, San Diego, CA, USA).

323 ## Results

324 **Desmoplakin is localized around the cell bodies of granule cells in the hippocampal**
325 **DG and is responsible for chronic antidepressant stimulation**

326 *Dsp,* a granule cell-specific maturation marker (Yamasaki et al., 2008; Kobayashi et al.,
327 2010), is highly and specifically expressed in the DG of the hippocampus of the central
328 nervous system (Supplemental Fig. 1, Allen Institute for Brain Science, 2004).
329 Although we previously observed that the gene expression level of Dsp significantly
330 decreased in the DG of mice treated with antidepressant stimulation (Kobayashi et al.,
331 2010; Imoto et al., 2017), the localization of Dsp in the DG was not confirmed.
332 Therefore, we initially examined the cellular localization and cell type of Dsp protein
333 expression. Immunohistological analysis revealed that Dsp was localized around the
334 cell bodies (Fig. 1A and 1C). Double immunohistochemical staining with Dsp and
335 NeuN showed that Dsp immunoreactivity signals were detected in NeuN-positive cells
336 in the outer DG, whereas Dsp signals were sparse in NeuN-negative and NeuN-positive
337 cells in the inner DG, which predominantly contains neuronal progenitors and immature
338 neurons (Fig. 1A [a], [b]). These findings suggest that Dsp is mostly localized in mature
339 granule cells in the DG. Dsp immunostaining was only observed after methanol
340 fixation; therefore, the localization of other neuronal markers was not investigated.

341 Furthermore, we investigated whether Dsp expression was regulated by
342 antidepressant stimulation at the protein level. The expression of *Dsp* was reduced by
343 chronic administration of electroconvulsive seizure (ECS) or a selective serotonin
344 reuptake inhibitor (SSRI) (Fig. 1B), as previously reported (Imoto et al., 2017).
345 Immunohistological analysis confirmed that the cellular localization of Dsp was
346 reduced after repeated administration of ECS (Fig. 1C).

347

348 **Dsp expression knockdown in the DG by an adeno-associated virus (AAV)**
349 **carrying Dsp miRNA**
350 To explore the role of Dsp in hippocampal function, we performed an AAV-mediated
351 knockdown of Dsp in the DG. For this purpose, we generated AAVrh10 expressing
352 EGFP and an artificial miRNA targeting Dsp mRNA (AAV-Dsp miRNA; Fig. 2A). The
353 AAV rh10 serotype shows high transduction efficiency into granule cells in the DG
354 (Sehara et al., 2022). Seven to eight weeks after the injection of AAV-Dsp or control
355 miRNA into the DG, EGFP signals, which were co-expressed with Dsp miRNA, were
356 observed in the granule cells but not in the immature neuronal marker DCX-positive
357 cells in the DG (Fig. 2A). *Dsp* mRNA expression significantly decreased in the AAV-
358 Dsp miRNA group (Fig. 2B). Moreover, immunohistological analysis showed a
359 decrease in Dsp immunoreactivity in the DG following AAV-Dsp miRNA injection
360 (Fig. 2C), demonstrating that the sequence of artificial miRNAs targeting Dsp used in
361 this study has the potential to knockdown Dsp expression.
362
363 **Changes in activity- and mature-related marker expression in the DG and**
364 **alteration the sensitivity to serotonin at the MF synapse by Dsp knockdown**
365 First, we examined the direct effect of Dsp knockdown on the activity of mature DG
366 neurons. FosB, including ΔFosB, is induced in response to many types of chronic
367 stimuli and accumulates because of its high stability (Nestler et al., 1999; Lamothe-
368 Molina et al., 2022). Consequently, we performed immunohistochemical analysis using
369 an anti-FosB antibody to monitor neuronal activity in the DG under normal home-cage
370 conditions. FosB immunoreactivity in the granule cell layer of the DG significantly
371 decreased in the Dsp knockdown group (Fig. 3A).

372 Because Dsp is a granule cell-specific DG maturation marker (Yamasaki et al.,
373 2008; Kobayashi et al., 2010), we examined the expression of other markers, including
374 *Calb, Tdo2, Ntf3, and Il1r1,* in the DG. The expression of *Calb, Tdo2,* and *Ntf3*
375 significantly increased in the DG of the Dsp knockdown group (Fig. 3B). These results
376 indicate that Dsp in the DG is involved in the regulation of neuronal activity and
377 expression of maturation markers.

378 Dsp interacts with the desmosomal component γ-catenin (plakoglobin). We
379 hypothesized that the loss of Dsp may regulate catenin-related transcription via
380 enhancement of γ-catenin translocation into the nucleus (Garcia-Gras et al., 2006).
381 Therefore, we examined the gene expression of *Hdac2* and *Tiam1*, which are subject to
382 transcriptional regulation by catenin, and found that their expression increased in the
383 Dsp knockdown group (Fig. 3C).

384 Antidepressant treatments substantially change the physiological properties of
385 the synapses formed by DG output MFs onto CA3 pyramidal cells, concomitantly with
386 the reduction in Dsp expression (Kobayashi et al., 2010; Imoto et al., 2017).
387 Electrophysiological analyses of MF-CA3 synaptic transmission were then performed
388 using acute hippocampal slices (Fig. 4A). No significant changes in the ratio of field
389 EPSP to fiber volleys were observed (Fig. 4B), suggesting that the basal transmission
390 efficacy at the MF synapse was not altered by Dsp knockdown. Antidepressant
391 treatment attenuates the synaptic facilitation induced by repetitive stimulation and
392 augments serotonergic modulation at the MF synapse (Kobayashi et al., 2010; Imoto et
393 al., 2017; Kobayashi et al., 2020). Dsp knockdown did not change synaptic facilitation
394 after 1 Hz stimulation (Fig. 4C and D). Bath-applied serotonin induced the potentiation
395 of field EPSPs in the AAV control group (Fig. 4E), consistent with the findings of
396 previous studies. The magnitude of serotonin-induced potentiation was significantly

397 reduced in the Dsp knockdown group (Fig. 4E and F). Collectively, these findings
398 indicate that suppression of Dsp alters neuronal activity in the DG and sensitivity to
399 serotonin at the MF synapse.
400
401 **Changes in neurogenic activity in the DG by Dsp knockdown**
402 The activation state of mature neurons in the DG affects the adjacent neurogenic
403 processes (Segi-Nishida and Suzuki, 2022). Since the above results suggest that Dsp in
404 mature DG neurons regulates neuronal activation, we explored the influence of Dsp
405 knockdown on hippocampal neurogenesis. Neurogenesis involves cell proliferation,
406 neuronal differentiation, and survival. First, we examined the effect of Dsp knockdown
407 on cell proliferation. BrdU was administered 2 h before the sacrifice to label
408 proliferating cells (Fig. 5A, left). BrdU-positive cells were detected in the SGZ of the
409 DG (Fig. 5A, middle), and no difference was observed in the number of proliferating
410 cells between the control and Dsp knockdown groups (Fig. 5A, right). We then
411 examined the expression of Neuro D1, which is expressed in progenitors/neuroblasts
412 and immature neurons in the adult DG. The number of NeuroD1-positive cells in the
413 SGZ was significantly decreased in the Dsp knockdown group (Fig. 5B). We further
414 examined the expression of the immature neuronal marker, DCX, in the DG. The total
415 number of DCX-positive cells and those with long dendrites decreased in the Dsp
416 knockdown group (Fig. 5C). Because most newborn cells in the DG die within 2–3
417 weeks following proliferation in mice (Ueno et al., 2019), we evaluated the effect of
418 Dsp knockdown on the survival of newborn cells 2 weeks after BrdU administration
419 (Fig. 5D, left). The number of BrdU-positive cells in the DG did not differ between the
420 control and Dsp knockdown groups (Fig. 5D, right).
421

422 **Influence of Dsp knockdown on anxiety-related behaviors**

423 The ventral DG is a key brain region involved in emotional behaviors, including
424 anxiety- and depression-like behaviors (Sahay and Hen, 2007; Levone et al. 2015;
425 Anacker et al. 2018). To examine the influence of Dsp knockdown in the DG on
426 emotion-related behaviors, we conducted three sets of behavioral experiments (Fig. 6A).
427 First, we performed an open-field test to assess behavior in an anxiety-provoking
428 environment. Dsp knockdown in the DG suppressed locomotor activity in the open field
429 box, and a suppressive trend was observed; however, it was not significant for the time
430 spent in the central area or the number of entries into the central area (Fig. 6B). Next,
431 we evaluated immobility time in the FST to assess depression-like behavior. No
432 difference in immobility time between the control and Dsp knockdown groups was
433 observed (Fig. 6C). Another set of experiments was conducted on locomotor activity in
434 a home cage, social interaction test, and elevated plus maze test. Contrary to the results
435 of the open field box, no change in locomotor activity between the control and
436 knockdown groups was observed (Fig. 6D), indicating normal locomotor activity under
437 ordinal circumstances and decreased locomotor activity in anxiety-provoking
438 environments following Dsp knockdown. In the three-chamber social interaction test,
439 the control mice spent more time around the area with an unfamiliar mouse than around
440 the area with empty cages. This social interaction behavior was comparable to that
441 observed in the Dsp knockdown mice (Fig. 6E). In the elevated plus maze test, a
442 reduction in both the time spent in the open arm and locomotor activity was observed
443 in Dsp knockdown mice (Fig. 6F). These results demonstrate that Dsp knockdown mice
444 in the DG shows anxiety-like behavior. Also, these findings can implicate that
445 expression of Dsp in the DG plays an anti-anxiety role.

Discussion

This study aimed to investigate the role of Dsp expressed in the DG in hippocampal function and emotion-related behaviors. We showed that Dsp is localized mostly in mature granule cells in the DG and that knockdown of Dsp decreases the expression of neuronal activity marker and serotonin responsiveness in DG neurons while enhancing the expression of mature neuronal markers. In addition, we demonstrated that Dsp knockdown in the DG impairs adult neurogenic processes in the adjacent SGZ and that these hippocampal changes contribute to anxiety-like behaviors. These findings suggest that Dsp in the DG maintains the activity of mature neurons, regulates neuronal differentiation in the adult neurogenic process, and contributes to anxiolytic effects. This study is the first to demonstrate the role of Dsp in neuronal activity and emotion-related behaviors in the DG.

Expression of desmoplakin in the DG

Since Dsp could play an important role in cell-to-cell adhesion and subsequent intracellular regulatory signaling, we initially confirmed its localization in the brain. In the central nervous system, *Dsp* was specifically expressed in the hippocampal DG (Supplemental Fig. 1). Immunohistological studies showed that Dsp was localized in the cell bodies of most dentate granule cells (Fig. 1A). Moreover, Dsp expression was lower in the inner DG than in the inner DG. *Dsp* expression in the adult DG was similar to that of the DG maturation markers *Calb* and *Tdo2* (Kobayashi et al., 2010), suggesting that Dsp is expressed in mature DG neurons. These results are consistent with those of a previous study that demonstrated that Dsp colocalizes with the post-mitotic neuron marker Bcl11b but not with the neural stem cell/progenitor marker SOX2 in the DG at 14 days of age (Simon et al., 2012).

471 Desmosome components include transmembrane cadherins and intracellular
472 proteins such as plakoglobin, plakophilin, and Dsp (Garrod and Chidgrey, 2008;
473 Broussard et al., 2015). Electron microscopy images of the rat DG showed no
474 desmosome structures between the cell bodies (Laatsch and Cowan, 1966). Therefore,
475 Dsp in the DG may form a complex different from that in epithelial desmosomes. The
476 expression and interactions of each desmosome component in the DG will be examined
477 to elucidate the localization and function of Dsp in neurons.
478
479 **Role of desmoplakin in mature DG neurons**
480 We found that Dsp knockdown in the DG suppressed FosB expression (Fig. 3A); FosB
481 is useful for monitoring steady-state activation since FosB, including ΔFosB, is induced
482 in response to many types of stimuli and shows high stability (Nestler et al., 1999;
483 Lamothe-Molina et al., 2022). In contrast, Dsp knockdown increased the expression of
484 the mature neuronal markers *Calb1*, *Tdo2*, and *Ntf3* (Fig. 3B), which are negatively
485 regulated by strong neuronal activation, such as in the ECS and epileptic seizures
486 (Imoto et al., 2017; You et al., 2017). Electrophysiological analysis showed that Dsp
487 suppression did not alter the basal transmission efficiency at the MF-CA3 synapses;
488 however, it reduced serotonin-induced potentiation (Fig. 4). Synaptic potentiation by
489 serotonin is mediated by presynaptic 5-HT4 receptor-cAMP signaling in the MF
490 (Kobayashi et al., 2008; 2020). Collectively, reduced neuronal activity due to Dsp
491 knockdown may enhance mature marker expression and alter serotonin-activated
492 intracellular signaling in the DG neurons.
493 Dsp is involved in processes such as gene expression, differentiation, and cell
494 migration (Bendrick et al., 2018; Dubash et al., 2016; Lombardi et al., 2016; Patel et
495 al., 2014). Dsp interacts with plakoglobin, also known as γ-catenin (Delva et al., 2009).

496 Suppression of Dsp expression in atrial myocyte cell lines leads to nuclear localization
497 of plakoglobin (Garcia-Gras et al., 2006). We showed that the expression of *Hdac2* and
498 *Tiam1*, which are transcriptionally regulated by catenin signaling, was increased by the
499 suppression of Dsp expression (Fig. 3C). HDAC2 negatively regulates gene expression
500 involved in synapse formation and synaptic plasticity in neurons (Guan et al., 2009;
501 Wang et al., 2018); Tiam1 is a Rho-guanine nucleotide exchange factor (Rho-GEF),
502 important for synaptic structure and function in the hippocampal DG (Rao et al., 2019).
503 Further detail analysis will be required to characterize the Dsp-mediated signaling
504 pathway. In addition, confirmation of the nuclear translocation of plakoglobin (γ-
505 catenin) will clarify whether changes in the expression of these factors are mediated by
506 catenin signaling.
507
508 **Influence of desmoplakin knockdown on the neurogenic process in the DG**
509 Adult neurogenesis occurs in the SGZ of the DG. Neurogenesis is regulated by various
510 signals from surrounding neurons (Kempermann et al., 2015). We investigated the role
511 of Dsp in the DG neurons in adult neurogenesis. Suppression of Dsp reduced the
512 number of NeuroD1-positive neural progenitors and DCX-positive immature neurons,
513 whereas the number of proliferating cells remained unchanged (Fig. 5). EGFP signals,
514 which were coexpressed with Dsp miRNA, were not observed in DCX-positive cells of
515 the DG (Fig. 2A), suggesting that Dsp in DG neurons indirectly regulates neurogenic
516 processes in the adjacent SGZ. Forebrain neuron-specific ablation of Dsp impairs
517 hippocampal neurogenesis on postnatal day 14 (Simon et al., 2012). During postnatal
518 development in this mutant line, cell proliferation was suppressed, whereas the number
519 of NeuroD1-positive progenitors increased. All these findings suggest that Dsp is
520 important for the regulation of cell proliferation during developmental neurogenesis

521 and for neural differentiation during both developmental and adult neurogenesis. The
522 reduction in the number of neural progenitors and immature neurons observed in this
523 study may be due to the inhibition of the initial process of neural differentiation or
524 acceleration of the differentiation rate, which allowed them to progress to maturity
525 without sufficient differentiation. Subsequent examination of neuronal differentiation
526 using surviving BrdU-labeled cells will clarify the role of Dsp in adult neurogenesis.
527 How does Dsp indirectly regulate neuronal differentiation in post-mitotic
528 neurons? Neuronal activation, such as that in the ECS, promotes the expression of adult
529 neurogenic factors such as *Vegf*, *Fgf2*, and *Wnt2* in the DG (Newton et al., 2003;
530 Warner-Schmidt et al., 2007). Therefore, the suppression of neuronal activity in the DG
531 by inhibiting Dsp expression may reduce the expression of these growth factors.
532 Furthermore, intracellular skeletal regulation by Dsp may also affect neurogenic niche
533 formation. The neurogenic niche provides a unique milieu containing an extracellular
534 matrix, humoral factors, and cell-cell contacts that allow controlled neuronal
535 development (Kempermann et al., 2015). Altering the cytoskeleton of dentate granule
536 cells may affect intercellular contacts and extracellular matrix adhesion and inhibit
537 neurogenic niche formation.
538
539 **Desmoplakin in the DG as a key regulator for emotion-related behaviors**
540 The DG of the hippocampus controls emotion-related behaviors (Segi-Nishida and
541 Suzuki, 2023). Although Dsp knockdown in the DG did not affect home cage activity,
542 depression-like behavior, or social behavior, it reduced the time spent in the open arm
543 in the EPM test and reduced activity in the novel open field and EPM environment (Fig.
544 6), indicating an anxious phenotype. The hippocampus plays functionally distinct roles
545 in the dorsal and ventral regions (Fanselow and Dong, 2010). The dorsal region is

546 involved in stress-induced learning and memory changes, and the ventral region
547 contributes to stress responses and emotions such as anxiety. Because AAV was injected
548 into the ventral DG area in this study (as described in the Methods section), Dsp in the
549 ventral DG may play an anxiolytic role.

550 Chronic antidepressant treatment induces anxiolytic-like effects (Santarelli et
551 al., 2003) and promotes the differentiation of newborn neurons in the DG (Wang et al.,
552 2008; Ueno et al., 2019), while suppressing the expression of mature markers, including
553 *Dsp,* in the DG (Fig. 1; Kobayashi et al., 2010; Imoto et al., 2017). The loss of Dsp
554 function in the DG may lead to anxiolytic effects; however, surprisingly, anxiety-like
555 behavior was observed (Fig. 6). Adult neurogenesis in the DG affects anxiety-like
556 behaviors. Transgenic mice in which adult neurogenesis was suppressed by the
557 expression of the pro-apoptotic protein BAX in neural progenitor cells show increased
558 anxiety-related behaviors (Revest et al., 2009). Therefore, suppression of adult
559 neurogenesis in the DG by Dsp knockdown may promote anxiety-like behaviors.

560 Furthermore, acute activation of the ventral DG by channelrhodopsin in
561 proopiomelanocortin (POMC)-Cre mice suppresses anxiety-like behavior in the EPM
562 (Kheirbek et al., 2013). Because our findings showed that Dsp knockdown in the DG
563 reduced the expression of the neuronal activity marker FosB (Fig. 3), the suppression
564 of neuronal activity in the DG by Dsp knockdown may also contribute to anxiety-like
565 behavior.

566 Taken together, our findings demonstrate that Dsp in the DG regulates neuronal
567 function and contributes to anxiolytic effects. This research uncovers an unexplored
568 function for Dsp in the central nervous system and implies that Dsp in the DG may
569 function as a regulator maintaining proper neuronal activation. Excessive
570 antidepressant treatment can exacerbate neuronal activation, resulting in increased

motor activity (Kobayashi et al., 2010; 2011). Considering the results of these studies and our findings, Dsp knockdown in the DG may function as a negative feedback mechanism for excessive neuronal activation rather than merely mimicking the effects of antidepressants or anxiolytics. This is because chronic antidepressant treatment reduces Dsp expression. Further studies are needed to investigate how Dsp knockdown alters stress-induced responsibility and emotion-related behaviors. Furthermore, the elucidation of the regulation of intracellular signaling by Dsp will enhance understanding of the development and neuronal function of the DG.

Data availability statement

All datasets analyzed in the current study are available from the corresponding author upon reasonable request.

Ethics statement

Animal use and procedures were conducted in accordance with the Tokyo University of Science regulations on animal care and use in research and were approved by the Animal Care and Use Committee of Tokyo University of Science (approval number K20009, K21007, and K22007).

Author contributions: KO, NS, YN, YS and KK designed the study, conducted the experiments, analyzed the data, and drafted the manuscript. KS designed the study and drafted the manuscript. ESN designed the study, analyzed the data, and drafted the manuscript. All the authors have read and approved the final manuscript.

Funding statements: This work was supported in part by MEXT KAKENHI Grants 20K07090 (ESN), 22K20697 (KS), 23H02801(KK and ESN), and 23K18425(KK). Kato Memorial Bioscience Foundation (KS), Brain Science Foundation (KS), Takeda Science Foundation (KS).

Conflict of interest: The authors have no potential conflicts of interest to declare relevant to this article.

Acknowledgements: We would like to thank *Editage* (www.editage.jp) for the English language editing.

References

Allen Institute for Brain Science (2004). Allen Mouse Brain Atlas [https://mouse.brain-map.org/experiment/show/69201504]. Available from mouse.brain-map.org.

Anacker, C., Luna, V.M., Stevens, G.S., Millette, A., Shores, R., Jimenez, J.C., Chen, B., and Hen, R. (2018). Hippocampal neurogenesis confers stress resilience by inhibiting the ventral dentate gyrus. *Nature* 559, 98-102. doi:10.1038/s41586-018-0262-4

Bendrick, J.L., Eldredge, L.A., Williams, E.I., Haight, N.B., and Dubash, A.D. (2019). Desmoplakin Harnesses Rho GTPase and p38 Mitogen-Activated Protein Kinase Signaling to Coordinate Cellular Migration. *J Invest Dermatol* 139, 1227-1236. doi:10.1016/j.jid.2018.11.032

Broussard, J.A., Getsios, S., and Green, K.J. (2015). Desmosome regulation and signaling in disease. *Cell Tissue Res* 360, 501-512. doi:10.1007/s00441-015-2136-5

Delva, E., Tucker, D.K., and Kowalczyk, A.P. (2009). The desmosome. *Cold Spring Harb Perspect Biol* 1, a002543. doi:10.1101/cshperspect.a002543

Drew, L.J., Fusi, S., and Hen, R. (2013). Adult neurogenesis in the mammalian hippocampus: why the dentate gyrus? *Learn Mem* 20, 710-729. doi:10.1101/lm.026542.112

Dubash, A.D., Kam, C.Y., Aguado, B.A., Patel, D.M., Delmar, M., Shea, L.D., and Green, K.J. (2016). Plakophilin-2 loss promotes TGF-beta1/p38 MAPK-dependent fibrotic gene expression in cardiomyocytes. *J Cell Biol* 212, 425-438. doi:10.1083/jcb.201507018

Fanselow, M.S., and Dong, H.W. (2010). Are the dorsal and ventral hippocampus functionally distinct structures? *Neuron* 65, 7-19. doi:10.1016/j.neuron.2009.11.031

Garcia-Gras, E., Lombardi, R., Giocondo, M.J., Willerson, J.T., Schneider, M.D., Khoury, D.S., and Marian, A.J. (2006). Suppression of canonical Wnt/beta-catenin signaling by nuclear plakoglobin recapitulates phenotype of arrhythmogenic right ventricular cardiomyopathy. *J Clin Invest* 116, 2012-2021. doi:10.1172/JCI27751

Garrod, D., and Chidgey, M. (2008). Desmosome structure, composition and function. *Biochim Biophys Acta* 1778, 572-587. doi:10.1016/j.bbamem.2007.07.014

Guan, J.S., Haggarty, S.J., Giacometti, E., Dannenberg, J.H., Joseph, N., Gao, J., Nieland, T.J., Zhou, Y., Wang, X., Mazitschek, R., Bradner, J.E., DePinho, R.A.,

Jaenisch, R., and Tsai, L.H. (2009). HDAC2 negatively regulates memory formation and synaptic plasticity. *Nature* 459, 55-60. doi:10.1038/nature07925

Imoto, Y., Segi-Nishida, E., Suzuki, H., and Kobayashi, K. (2017). Rapid and stable changes in maturation-related phenotypes of the adult hippocampal neurons by electroconvulsive treatment. *Mol Brain* 10, 8. doi:10.1186/s13041-017-0288-9

Johnson, J.L., Najor, N.A., and Green, K.J. (2014). Desmosomes: regulators of cellular signaling and adhesion in epidermal health and disease. *Cold Spring Harb Perspect Med* 4, a015297. doi:10.1101/cshperspect.a015297

Kempermann, G., Song, H., and Gage, F.H. (2015). Neurogenesis in the Adult Hippocampus. *Cold Spring Harb Perspect Biol* 7, a018812. doi:10.1101/cshperspect.a018812

Kheirbek, M.A., Drew, L.J., Burghardt, N.S., Costantini, D.O., Tannenholz, L., Ahmari, S.E., Zeng, H., Fenton, A.A., and Hen, R. (2013). Differential control of learning and anxiety along the dorsoventral axis of the dentate gyrus. *Neuron* 77, 955-968. doi:10.1016/j.neuron.2012.12.038

Kobayashi, K., Ikeda, Y., Haneda, E., and Suzuki, H. (2008). Chronic fluoxetine bidirectionally modulates potentiating effects of serotonin on the hippocampal mossy fiber synaptic transmission. *J Neurosci* 28, 6272-6280. doi:10.1523/JNEUROSCI.1656-08.2008

Kobayashi, K., Ikeda, Y., Sakai, A., Yamasaki, N., Haneda, E., Miyakawa, T., and Suzuki, H. (2010). Reversal of hippocampal neuronal maturation by serotonergic antidepressants. *Proc Natl Acad Sci U S A* 107, 8434-8439. doi:10.1073/pnas.0912690107

Kobayashi, K., Ikeda, Y., and Suzuki, H. (2011). Behavioral destabilization induced by the selective serotonin reuptake inhibitor fluoxetine. *Mol Brain* 4, 12. doi:10.1186/1756-6606-4-12

Kobayashi, K., Mikahara, Y., Murata, Y., Morita, D., Matsuura, S., Segi-Nishida, E., and Suzuki, H. (2020). Predominant Role of Serotonin at the Hippocampal Mossy Fiber Synapse with Redundant Monoaminergic Modulation. *iScience* 23, 101025. doi:10.1016/j.isci.2020.101025

Kowalczyk, A.P., and Green, K.J. (2013). Structure, function, and regulation of desmosomes. *Prog Mol Biol Transl Sci* 116, 95-118. doi:10.1016/B978-0-12-394311-8.00005-4

Laatsch, R.H., and Cowan, W.M. (1966). Electron microscopic studies of the dentate gyrus of the rat. I. Normal structure with special reference to synaptic organization. *J Comp Neurol* 128, 359-395. doi:10.1002/cne.901280305

Lamothe-Molina, P.J., Franzelin, A., Beck, L., Li, D., Auksutat, L., Fieblinger, T., Laprell, L., Alhbeck, J., Gee, C.E., Kneussel, M., Engel, A.K., Hilgetag, C.C., Morellini, F., and Oertner, T.G. (2022). DeltaFosB accumulation in hippocampal granule cells drives cFos pattern separation during spatial learning. *Nat Commun* 13, 6376. doi:10.1038/s41467-022-33947-w

Levone, B.R., Cryan, J.F., and O'Leary, O.F. (2015). Role of adult hippocampal neurogenesis in stress resilience. *Neurobiol Stress* 1, 147-155. doi:10.1016/j.ynstr.2014.11.003

Lombardi, R., Chen, S.N., Ruggiero, A., Gurha, P., Czernuszewicz, G.Z., Willerson, J.T., and Marian, A.J. (2016). Cardiac Fibro-Adipocyte Progenitors Express Desmosome Proteins and Preferentially Differentiate to Adipocytes Upon Deletion of the Desmoplakin Gene. *Circ Res* 119, 41-54. doi:10.1161/CIRCRESAHA.115.308136

Nestler, E.J., Kelz, M.B., and Chen, J. (1999). DeltaFosB: a molecular mediator of long-term neural and behavioral plasticity. *Brain Res* 835, 10-17. doi:10.1016/s0006-8993(98)01191-3

Newton, S.S., Collier, E.F., Hunsberger, J., Adams, D., Terwilliger, R., Selvanayagam, E., and Duman, R.S. (2003). Gene profile of electroconvulsive seizures: induction of neurotrophic and angiogenic factors. *J Neurosci* 23, 10841-10851. doi:10.1523/JNEUROSCI.23-34-10841.2003

Patel, D.M., Dubash, A.D., Kreitzer, G., and Green, K.J. (2014). Disease mutations in desmoplakin inhibit Cx43 membrane targeting mediated by desmoplakin-EB1 interactions. *J Cell Biol* 206, 779-797. doi:10.1083/jcb.201312110

Paxinos, G.F., K. B. J., 2012. 4th ed. Academic Press., Cambridge, MA.

Rao, S., Kay, Y., and Herring, B.E. (2019). Tiam1 is Critical for Glutamatergic Synapse Structure and Function in the Hippocampus. *J Neurosci* 39, 9306-9315. doi:10.1523/JNEUROSCI.1566-19.2019

Revest, J.M., Dupret, D., Koehl, M., Funk-Reiter, C., Grosjean, N., Piazza, P.V., and Abrous, D.N. (2009). Adult hippocampal neurogenesis is involved in anxiety-related behaviors. *Mol Psychiatry* 14, 959-967. doi:10.1038/mp.2009.15

Sahay, A., and Hen, R. (2007). Adult hippocampal neurogenesis in depression. *Nat Neurosci* 10, 1110-1115. doi:10.1038/nn1969

Santarelli, L., Saxe, M., Gross, C., Surget, A., Battaglia, F., Dulawa, S., Weisstaub, N., Lee, J., Duman, R., Arancio, O., Belzung, C., and Hen, R. (2003). Requirement of hippocampal neurogenesis for the behavioral effects of antidepressants. *Science* 301, 805-809. doi:10.1126/science.1083328

Segi-Nishida, E., and Suzuki, K. (2022). Regulation of adult-born and mature neurons in stress response and antidepressant action in the dentate gyrus of the hippocampus. *Neurosci Res*. doi:10.1016/j.neures.2022.08.010

Sehara, Y., Hayashi, Y., Ohba, K., Uchibori, R., Urabe, M., Inutsuka, A., Shimazaki, K., Kawai, K., and Mizukami, H. (2022). Higher Transduction Efficiency of AAV5 to Neural Stem Cells and Immature Neurons in Gerbil Dentate Gyrus Compared to AAV2 and rh10. *Hum Gene Ther* 33, 76-85. doi:10.1089/hum.2021.106

Shinohara, R., Taniguchi, M., Ehrlich, A.T., Yokogawa, K., Deguchi, Y., Cherasse, Y., Lazarus, M., Urade, Y., Ogawa, A., Kitaoka, S., Sawa, A., Narumiya, S., and Furuyashiki, T. (2018). Dopamine D1 receptor subtype mediates acute stress-induced dendritic growth in excitatory neurons of the medial prefrontal cortex and contributes to suppression of stress susceptibility in mice. *Mol Psychiatry* 23, 1717-1730. doi:10.1038/mp.2017.177

Simon, R., Brylka, H., Schwegler, H., Venkataramanappa, S., Andratschke, J., Wiegreffe, C., Liu, P., Fuchs, E., Jenkins, N.A., Copeland, N.G., Birchmeier, C., and Britsch, S. (2012). A dual function of Bcl11b/Ctip2 in hippocampal neurogenesis. *EMBO J* 31, 2922-2936. doi:10.1038/emboj.2012.142

Ueno, M., Sugimoto, M., Ohtsubo, K., Sakai, N., Endo, A., Shikano, K., Imoto, Y., and Segi-Nishida, E. (2019). The effect of electroconvulsive seizure on survival, neuronal differentiation, and expression of the maturation marker in the adult mouse hippocampus. *J Neurochem* 149, 488-498. doi:10.1111/jnc.14691

Wang, H., Warner-Schmidt, J., Varela, S., Enikolopov, G., Greengard, P., and Flajolet, M. (2015). Norbin ablation results in defective adult hippocampal neurogenesis and depressive-like behavior in mice. *Proc Natl Acad Sci U S A* 112, 9745-9750. doi:10.1073/pnas.1510291112

Wang, J.W., David, D.J., Monckton, J.E., Battaglia, F., and Hen, R. (2008). Chronic fluoxetine stimulates maturation and synaptic plasticity of adult-born hippocampal granule cells. *J Neurosci* 28, 1374-1384. doi:10.1523/JNEUROSCI.3632-07.2008

Wang, S.E., Ko, S.Y., Kim, Y.S., Jo, S., Lee, S.H., Jung, S.J., and Son, H. (2018). Capsaicin upregulates HDAC2 via TRPV1 and impairs neuronal maturation in mice. *Exp Mol Med* 50, e455. doi:10.1038/emm.2017.289

Warner-Schmidt, J.L., and Duman, R.S. (2007). VEGF is an essential mediator of the neurogenic and behavioral actions of antidepressants. *Proc Natl Acad Sci U S A* 104, 4647-4652. doi:10.1073/pnas.0610282104

Yamasaki, N., Maekawa, M., Kobayashi, K., Kajii, Y., Maeda, J., Soma, M., Takao, K., Tanda, K., Ohira, K., Toyama, K., Kanzaki, K., Fukunaga, K., Sudo, Y., Ichinose, H., Ikeda, M., Iwata, N., Ozaki, N., Suzuki, H., Higuchi, M., Suhara, T., Yuasa, S., and Miyakawa, T. (2008). Alpha-CaMKII deficiency causes immature dentate gyrus, a novel candidate endophenotype of psychiatric disorders. *Mol Brain* 1, 6. doi:10.1186/1756-6606-1-6

You, J.C., Muralidharan, K., Park, J.W., Petrof, I., Pyfer, M.S., Corbett, B.F., LaFrancois, J.J., Zheng, Y., Zhang, X., Mohila, C.A., Yoshor, D., Rissman, R.A., Nestler, E.J., Scharfman, H.E., and Chin, J. (2017). Epigenetic suppression of hippocampal calbindin-D28k by DeltaFosB drives seizure-related cognitive deficits. *Nat Med* 23, 1377-1383. doi:10.1038/nm.4413

Zhao, C., Deng, W., and Gage, F.H. (2008). Mechanisms and functional implications of adult neurogenesis. *Cell* 132, 645-660. doi:10.1016/j.cell.2008.01.033

Table 1. List of primers used for qPCR analysis.

Gene	Forward (5' to 3')	Reverse (5' to 3')
Dsp	GCTGAAGAACACTCTAGCCCA	ACTGCTGTTTCCTCTGAGACA
Calb1	TCTGGCTTCATTTCGACGCTG	ACAAAGGATTTCATTTCCGGTGA
Tdo2	ATGAGTGGGTGCCCGTTTG	GGCTCTGTTTACACCAGTTTGAG
Ntf3	AGTTTGCCGGAAGACTCTCTC	GGGTGCTCTGGTAATTTTCCTTA
Il1r1	GTGCTACTGGGGCTCATTTGT	GGAGTAAGAGGACACTTGCGAAT
Hdac2	GGAGGAGGCTACACAATCCG	TCTGGAGTGTTCTGGTTTGTCA
Tiam1	AGACTGAACGCACCTATGTGA	ACTCGACTTGAAACTCCACCAT
18S	GAGGCCCTGTAATTGGAATGAG	GCAGCAACTTTAATATACGCTATTGG
Gapdh	AGGTCGGTGTGAACGGATTTG	TGTAGACCATGTAGTTGAGGTCA

Figure 1

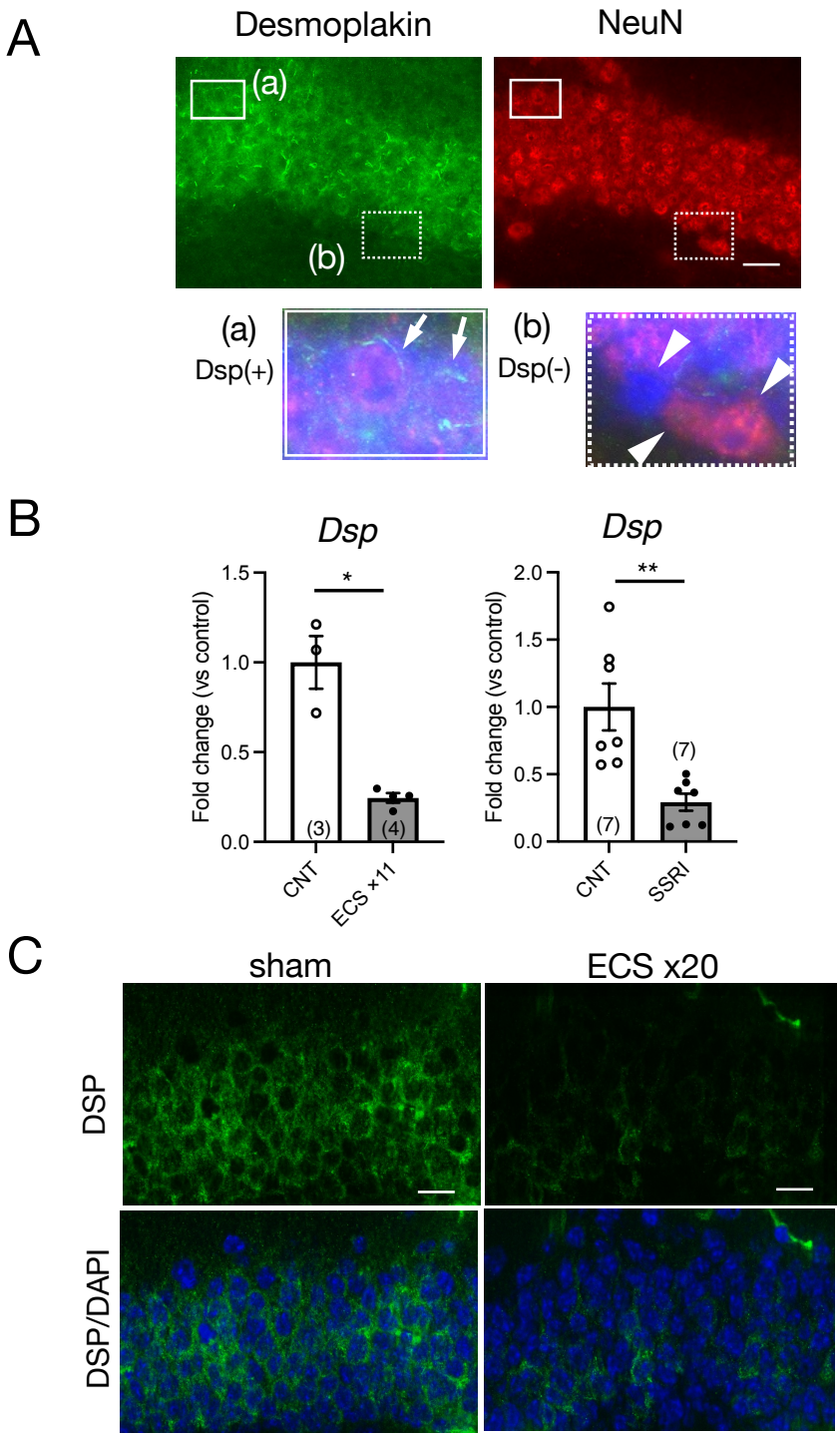

Figure 1. Expression of Dsp in the dentate gyrus (DG) of the hippocampus

(A) Representative images of immunoreactivity for Dsp (green) and NeuN (red) in the DG. Magnified images showing Dsp-positive (a; arrows) or -negative (b; arrowheads) cells. DAPI (blue) is utilized for nuclear staining. (B) Relative gene expression of *Dsp* at 24 h after 11 times of electroconvulsive seizure (ECS) stimulation (left) or 4-weeks treatment of selective serotonin reuptake inhibitor (SSRI) fluoxetine. Data are expressed using dot plots and means ± standard error of mean. *, $P<0.05$; **, $P<0.01$. The n number is given in graph. (C) Representative images of immunoreactivity for Dsp (DSP; green), and DAPI (blue) in the DG after 20 times of ECS stimulation. Scale bars: 20 μm.

Figure 2

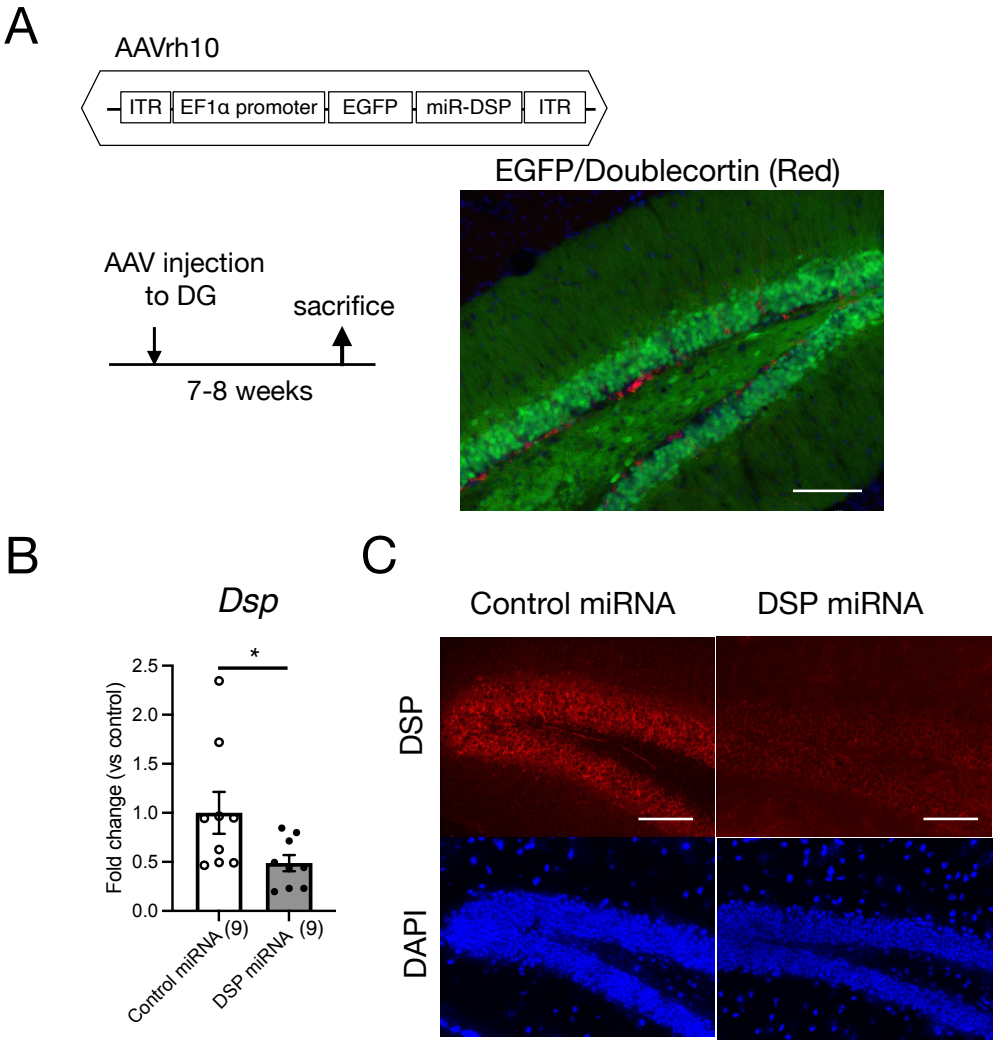

Figure 2. Knockdown of Dsp in the DG by adeno-associated virus (AAV) carrying Dsp artificial miRNA

(A) Structure of AAVrh10 carrying EGFP and artificial microRNA sequence for Dsp (DSP miRNA). Time course of experimental procedure (Left). EGFP and immunoreactivity for an immature neuronal marker doublecortin (red) in the DG indicating mature neuronal infection of the AAV after 7–8 weeks of injection. (B) Gene expression of *Dsp* 7–8 weeks after AAV infection. Data are expressed using dot plots and means ± standard error of mean. *, $P<0.05$. The n number is given in graph. (C) Representative images of immunoreactivity for Dsp (DSP; red) and DAPI (blue) in the DG 7–8 weeks after AAV infection. Scale bars: 100 μm.

Figure 3

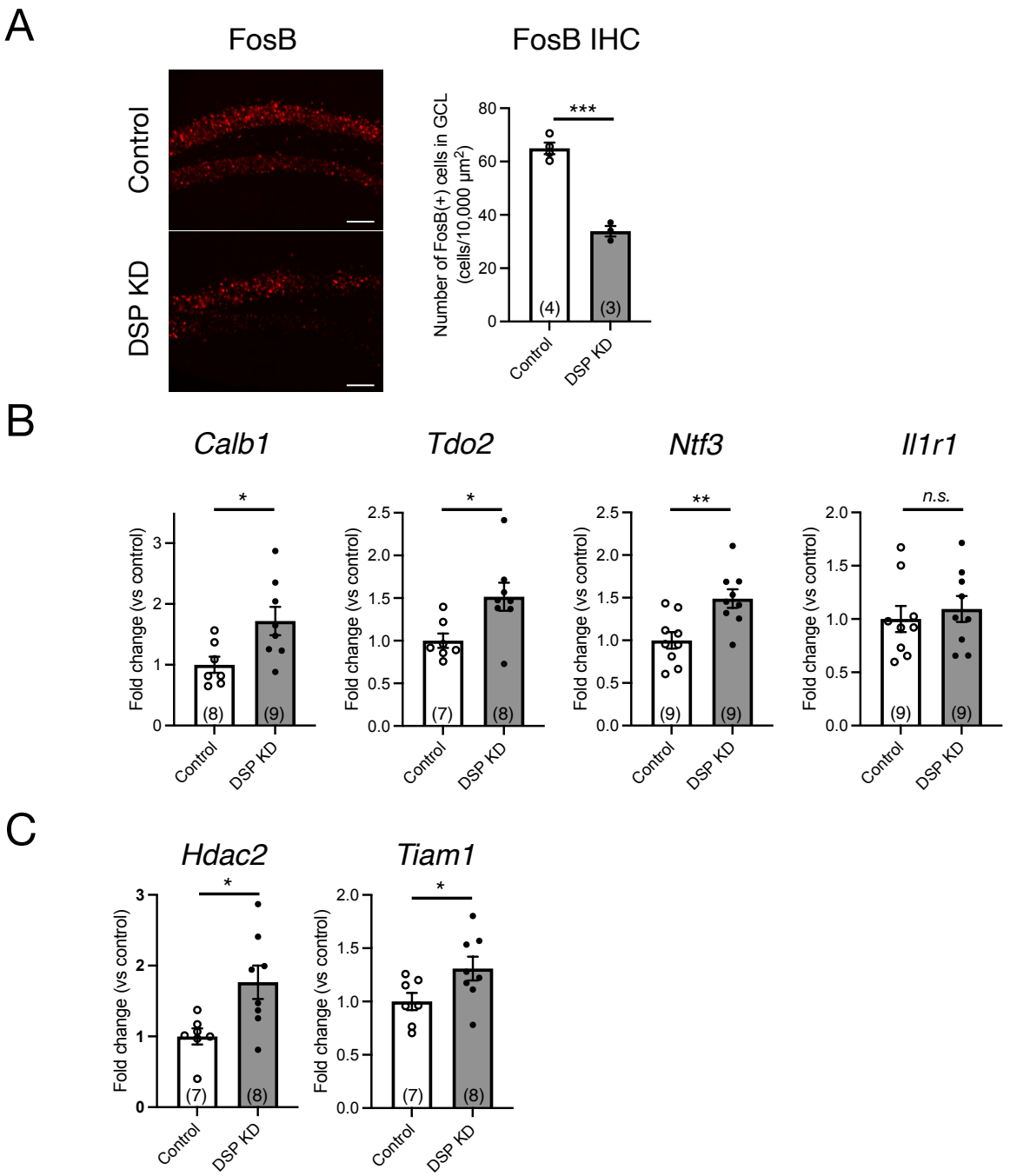

Figure 3. Expression changes in the DG by Dsp knockdown

(A) Effect of Dsp knockdown in the DG on the expression of FosB protein. Representative images of immunoreactivity for FosB in the DG (left). Scale bars: 100 μm. Quantification of FosB-positive cell numbers (right) in the granule cell layer. (B) Effect of Dsp knockdown in the DG on the expression of maturation markers in the DG. Expression of *Calb1, Tdo2, Ntf3,* and *Il1r1*. (C) Effect of Dsp knockdown in the DG on the expression of *Hdac2* and *Tiam1* which are regulated by β-catenin signaling in the DG. Data are expressed using dot plots and means ± standard error of mean. The n number is given in graph. *, $P<0.05$; **, $P<0.01$; ***, $P<0.001$; n.s., not significant.

Figure 4

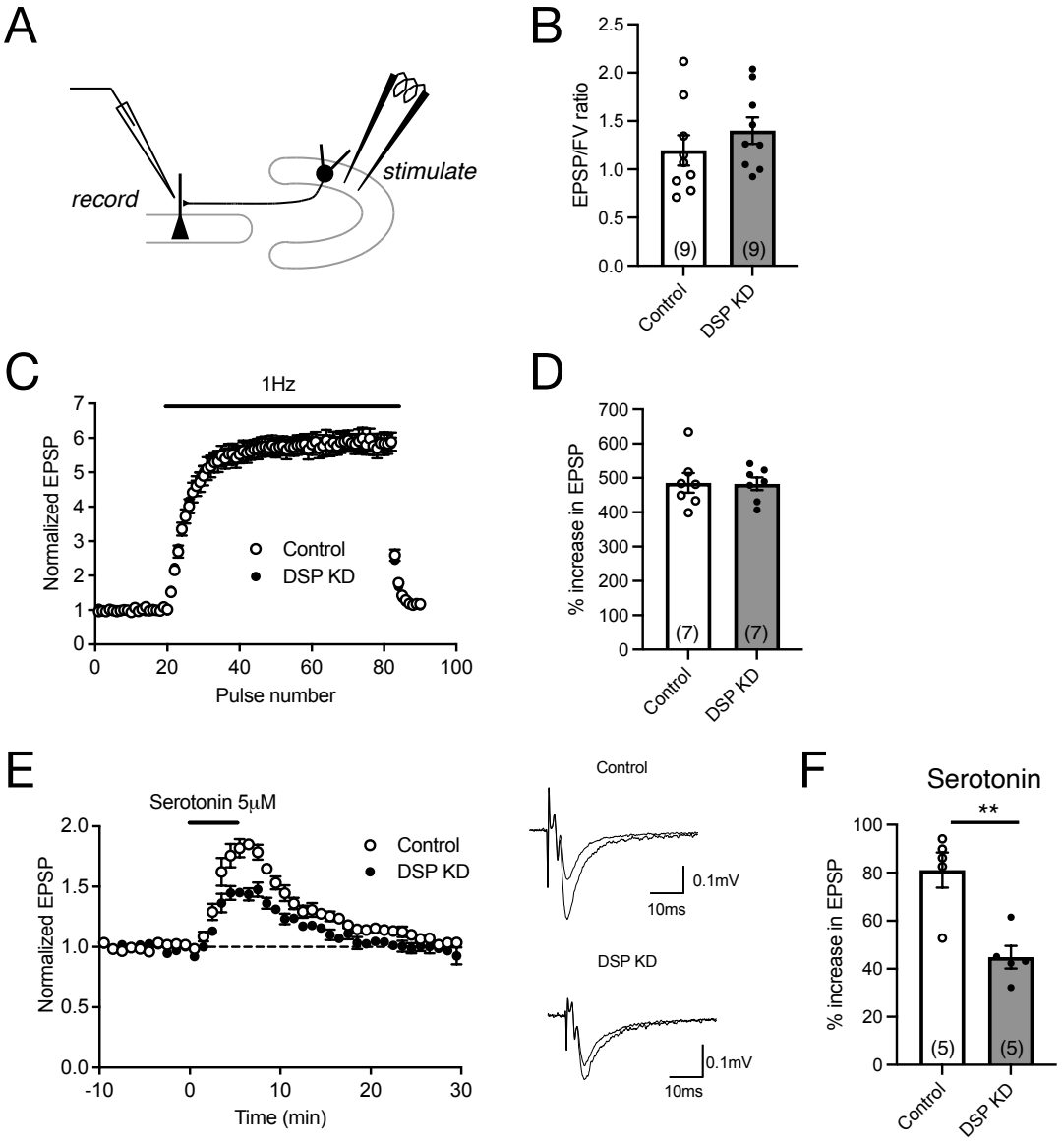

Figure 4. Electrophysiological changes in the DG by Dsp knockdown

(A) Diagram showing the electrode arrangement for recording field excitatory post synaptic potentials (EPSPs) at the mossy fiber (MF)–CA3 synapse. (B) Ratios for MF field EPSPs to fiber volley (FV) at the baseline stimulus intensity. (C and D) Effect of Dsp knockdown on synaptic facilitation induced by repetitive stimulation at the MF synapse. (E) Effect of Dsp knockdown on potentiation of MF synaptic transmission induced by serotonin (5 μM, 5 min) applied in the bath. Sample recordings show averages of nine consecutive field EPSPs before and at the end of serotonin application in control DG and knockdown DG. (F) Effect of Dsp knockdown on serotonin-induced synaptic potentiation. Data are expressed using dot plots and means ± standard error of mean. The n number of data given in graph represents the number of slices. **, $P<0.01$.

Figure 5

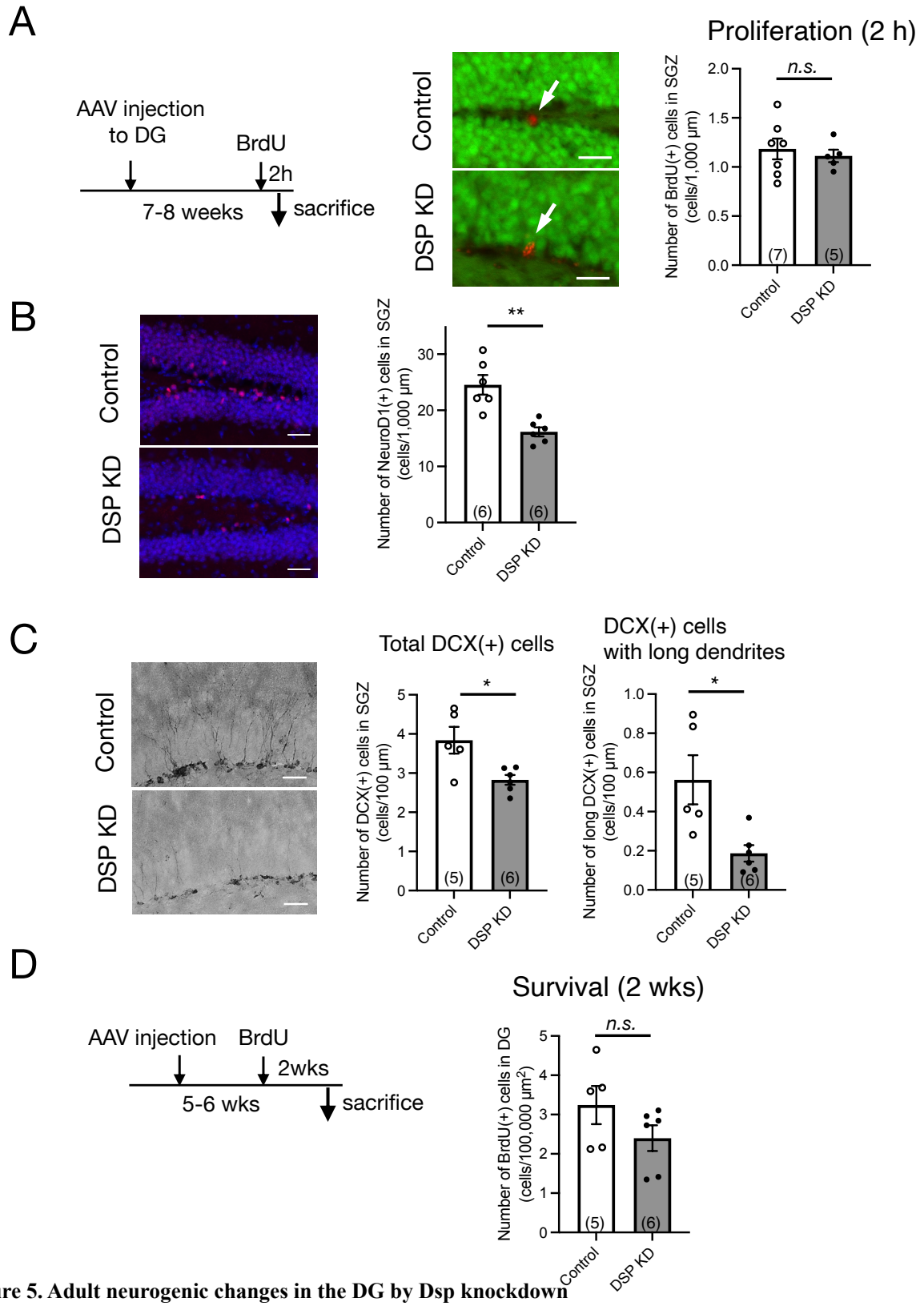

Figure 5. Adult neurogenic changes in the DG by Dsp knockdown
(A) Effect of Dsp knockdown on proliferation in the DG. Left: Time course of the experimental procedure. Middle: Representative images of immunoreactivity for BrdU. The arrows represent BrdU-positive cells in the SGZ. Scale bars: 20 μm. Right: Quantification of BrdU-positive cell numbers in the SGZ. (B) Effect of Dsp knockdown on neuronal differentiation in the DG. Left: Representative images of immunoreactivity for NeuroD1 in the DG. Scale bars: 100 μm. Right: Quantification of NeuroD1-positive cell numbers in the SGZ. (C) Effect of Dsp knockdown on cell number of doublecortin (DCX)-positive immature neurons in the DG. Left: Representative images of immunoreactivity for DCX in the DG. Scale bars: 40 μm. Middle: Quantification of DCX-positive cell numbers in the SGZ. Right: Quantification of DCX-positive cells with long dendrites in the SGZ. (D) Effect of Dsp knockdown on survival of 2-weeks of cell age in the DG. Left: Time course of the experimental procedure. Right: Quantification of BrdU-positive cells of 2-weeks (2 wks) of cell age in the DG. Data are expressed using dot plots and means ± standard error of mean. The n number is given in graph. *, $P<0.05$; **, $P<0.01$. n.s. not significant.

Figure 6

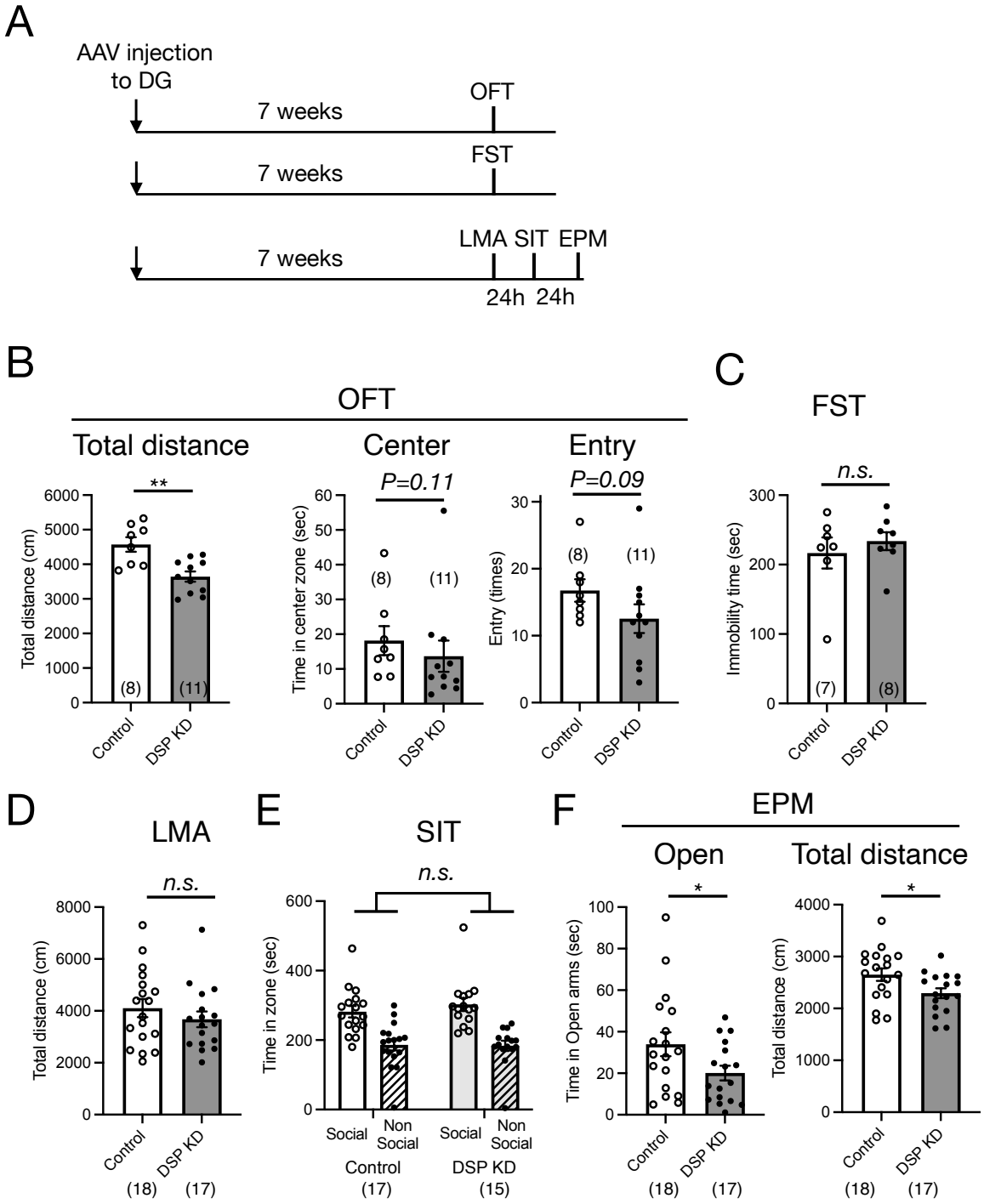

Figure 6. Behavioral changes in the DG by Dsp knockdown

(A) Time course of the experimental procedure. (B) Exploratory behaviors of open field test (OFT). Total distance (left) in the open field. Time spent (middle) and entry times (right) in the center of the open field. (C) Immobility time in the forced swim test (FST). (D) Total distance of locomotor activity (LMA) in the home cage. (E) Social interaction behavior in the 3-chamber social interaction test (SIT). A stranger mouse within a wire cup placed in one chamber (social) and an empty wire cup placed in another chamber (Non-Social). (F) Time spent on the open arms (left) and total distance (right) in the elevate plus maze (EPM) test. Data are expressed using dot plots and means ± standard error of mean. The n number is given in graph. *, $P<0.05$; **, $P<0.01$; n.s. not significant.